

11-16-2003

Substrate-Based Inhibitors of Peptidylglycine α -Amidating Monooxygenase (PAM) as Anti-Proliferative Drugs for Cancer

Geoffrey H. Chew
University of South Florida

Follow this and additional works at: <https://digitalcommons.usf.edu/etd>



Part of the [American Studies Commons](#)

Scholar Commons Citation

Chew, Geoffrey H., "Substrate-Based Inhibitors of Peptidylglycine α -Amidating Monooxygenase (PAM) as Anti-Proliferative Drugs for Cancer" (2003). *USF Tampa Graduate Theses and Dissertations*.
<https://digitalcommons.usf.edu/etd/1341>

This Thesis is brought to you for free and open access by the USF Graduate Theses and Dissertations at Digital Commons @ University of South Florida. It has been accepted for inclusion in USF Tampa Graduate Theses and Dissertations by an authorized administrator of Digital Commons @ University of South Florida. For more information, please contact digitalcommons@usf.edu.

Substrate-Based Inhibitors of Peptidylglycine α -Amidating
Monooxygenase (PAM) as Anti-Proliferative Drugs for Cancer

by

Geoffrey H. Chew

A thesis submitted in partial fulfillment
of the requirements for the degree of
Master of Science
Department of Chemistry
College of Arts and Sciences
University of South Florida

Major Professor: David Merkler, Ph.D.
Randy Larsen, Ph.D.
Gloria Ferreira, Ph.D.

Date of Approval:
November 16, 2003

Keywords: enzyme, prostate, inhibition, 4-hpr, kinetics

© Copyright 2003, Geoffrey H. Chew

Table of Contents

List of Tables	iii
List of Figures	iv
List of Graphs	v
Abstract	vi
Chapter One - Literature Review	1
Peptidylglycine α -amidating monooxygenase	1
Prostate cancer	5
Conclusion	8
Chapter Two - Novel Compounds for PAM	9
Introduction	9
<i>Enzyme inhibition</i>	9
<i>N-Benzoylglycine (hippuric acid) as lead compound</i>	11
<i>Methods to assay for PAM activity</i>	11
Experimental Procedures	13
<i>Materials</i>	13
<i>High-performance liquid chromatography</i>	14
<i>HPLC separation of dansylated compounds</i>	14
<i>Determination of initial rates of N-dansyl-Tyr-Val-NH₂ production as fixed N-dansyl-Tyr-Val-Gly concentration as a function of inhibitor concentration (Dixon analysis)</i>	15
<i>Determination of K_M and V_{MAX} values for N-dansyl-Tyr-Val-Gly as a function of inhibitor concentration</i>	16
<i>Determination of initial rates by oxygen consumption</i>	16
<i>Copper chelating experiment</i>	17
<i>Molecular Modeling</i>	17
Results and Discussion	18
<i>PAM substrates and inhibitors</i>	18
<i>Copper chelating experiment</i>	27
<i>Determination of K_M and V_{MAX} values for N-dansyl-Tyr-Val-Gly as a function of inhibitor concentration</i>	27

Conclusion	29
Chapter Three - Prostate Cancer Testing	31
Introduction	31
Experimental Procedures	32
<i>Materials</i>	32
<i>Cells and cell culture</i>	32
<i>Anti-proliferation assay of S-(4-methylthiobenzoyl)thioglycolic acid</i>	33
<i>Anti-proliferation assay of S-(phenylthioacetyl)thioglycolic acid</i>	33
Results and Discussion	34
<i>Anti-proliferation assay of S-(4-methylthiobenzoyl)thioglycolic acid</i>	34
<i>Anti-proliferation assay of S-(phenylthioacetyl)thioglycolic acid</i>	35
Conclusion	37
References	39

List of Tables

Table 1.	Kinetic parameters for <i>N</i> -dansyl-(Gly) ₄ -X-Gly amidation	5
Table 2.	List of PAM inhibitors	19
Table 3.	List of PAM substrates	20
Table 4.	Summary of bond energies	23
Table 5.	Comparison of inhibitor and substrate bond energies and binding constants	24
Table 6.	Comparison of substrates between the two assays	26

List of Figures

Figure 1.	The PAM catalyzed reaction	2
Figure 2.	3D structure of PHM with bound substrate	3
Figure 3.	Sequence comparison of PHM and DBM	4
Figure 4.	Structure of 4-HPR	7
Figure 5.	Diagram of three main types of inhibition	10
Figure 6.	Diagram of irreversible inhibition	10
Figure 7.	Sites of different binding energies	21
Figure 8.	Formula for calculating free energies for the complete docking of a compound into the active site of PHM	22

List of Graphs

Graph 1.	PAM activity in different prostate cancers	6
Graph 2.	PAM growth curve with AM	6
Graph 3.	PAM growth curve with 4-HPR	8
Graph 4.	Copper chelating experiment with EDTA	28
Graph 5.	Full kinetic study on S-(3-phenyl thiopropionyl)thioglycolic acid	29
Graph 6.	Full kinetic study on octanoyl glycine	30
Graph 7.	Anti-proliferative assay of S-(4-methylthiobenzoyl)thioglycolic acid	35
Graph 8.	Anti-proliferative assay of S-(phenylthioacetyl)thioglycolic acid	36

Substrate-Based Inhibitors of Peptidylglycine α -Amidating
Monooxygenase (PAM) as Anti-Proliferative Drugs for Cancer

Geoffrey H. Chew

ABSTRACT

C-Terminal glycine-extended prohormones are enzymatically converted to α -amidated peptides, by peptidylglycine α -amidating monooxygenase (PAM). PAM is a bifunctional enzyme with two catalytic domains: peptidylglycine α -hydroxylating monooxygenase (PHM) and peptidylglycine peptidylglycineaminoglycolate lyase (PAL).

PAM has a significant role in the proliferation of androgen-independent prostate cancer. Thus, the inhibition of PAM could halt cancer growth. Hippurate and hippurate analogs were used as lead compounds for developing inhibitors for PAM. The hippurate analogs exhibiting the highest affinity to PAM (lowest inhibition constant) did inhibit the growth of human androgen-independent prostate cancer DU 145 cells.

Chapter One

Literature Review

Peptidylglycine α -amidating monooxygenase

Approximately 50% of all mammalian hormones are amidated, and play important roles in biological systems. Many hormones, such as human growth hormone-releasing factor (GRF), are only active in the amidated form (Merkler 1994). C-Terminal glycine-extended prohormones are enzymatically converted to α -amidated peptides, by peptidylglycine α -amidating monooxygenase (PAM). PAM is the only known enzyme that performs this chemistry (Eipper 1988).

PAM enables the oxidative cleavage of inactive C-terminal glycine-extended prohormones to active α -amidated peptides and glyoxylate. PAM is a bifunctional enzyme with two catalytic domains: peptidylglycine α -hydroxylating monooxygenase (PHM) and peptidylamidoglycolate lyase (PAL) (Merkler, 1995). PHM catalyzes the O₂-, copper-, and ascorbate-dependent insertion of oxygen from an O₂ molecule at the C _{α} of the terminal glycyl residue to form a carbinolamide while PAL catalyzes the zinc-dependent dealkylation of the carbinolamide to the α -amidated peptide and glyoxylate (Jaron, 2002) (Figure 1).

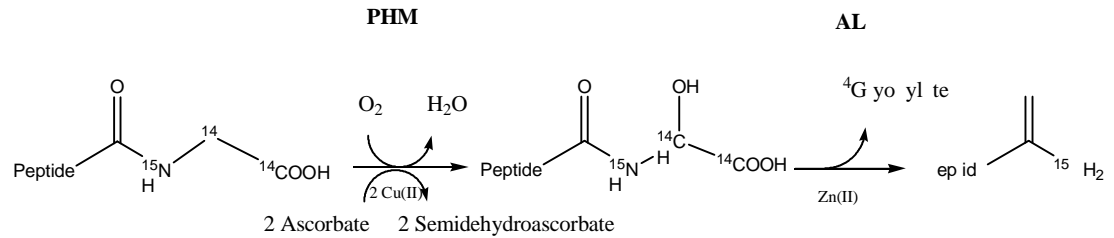


Figure 1-The peptide amidation reaction as catalyzed by PAM. PAM is a bifunctional protein comprised of two distinct catalytic entities: peptidylglycine α -hydroxylating monooxygenase (PHM) and peptidylamidoglycolate lyase (PAL). Labeled nitrogens and carbons were used in experiments to determine products of the reaction.

Early work performed using bifunctional PAM defined essential characteristics of the peptide amidation reaction. Incubation of D-Tyr-Val-[glycyl- ^{15}N]-Gly with bifunctional PAM yields D-Tyr-Val-[^{15}N]-NH₂, which demonstrates the glycyl nitrogen is retained in the final amide (Bradbury 1982). In a similar experiment, D-Tyr-Val-[^{14}C]-Gly was used as a substrate. The labeled carbon atoms were incorporated only into glyoxylate. Eipper et al. (1983) showed that molecular oxygen, copper, and an electron donor were required for the PAM reaction to occur. Metal chelators completely abolished PAM activity that only could be restored upon the addition of copper -- at a slight excess over the residual chelator concentration. The turnover of each glycine-extended peptide to the α -amidated peptide requires the input of two electrons, which can be donated from many different reductants. Ascorbic acid is the most efficient electron donor, exhibiting the highest $(V_{\text{MAX}}/K_{\text{M}})_{\text{app}}$ at constant peptide substrate concentration, and is likely the reductant utilized by PAM *in vivo* (Merkler 1992). After the discovery that PAM is bifunctional and that the C-terminal α -hydroxyglycine extended peptides are intermediates in the amidation reaction, it was established that O₂-, copper, and ascorbate were only required for the PHM reaction. Figure 2 shows the 3D structure of PHM with a bound substrate. Note the presence of two PHM-bound copper atoms, one on either side of the binding pocket.



Figure 2- 3D structure of PHM with bound substrate.

EPR studies performed by Freeman et al. (1993) demonstrated that PHM-bound Cu (II) redox cycles from Cu (II) to Cu (I) back to Cu (II) during catalysis. All of the copper ions before the addition of ascorbate are spin active. After the addition of ascorbate, 95% is no longer spin active, which indicated that the Cu (II) is reduced to Cu (I). After reaction with the substrate, Cu (I) reverts back to Cu (II).

PHM and dopamine α -monooxygenase (DBM) exhibit a number of catalytic similarities. Both enzymes insert an oxygen atom from O₂ into an inactivated C-H bond, have a copper stoichiometry of two copper atoms per active site, and oxidize two ascorbate molecules to semihydroascorbate per enzyme turnover. In addition to catalytic similarities, the two enzymes have similar protein sequence (Figure 3) and expression levels.

```

PVTPLDASDFALDIRMPGVT-PKESDITYFCMSMLRPVD-----EEAFVIDFKPRASM 103
P P D +DIR P V TY+C LP+ EA V + +
PAMPADVQ--TMDIRAPDVLIPSTETTYWCYITELPLHFPRHHIIMYEAIIVTE----GNE 76

DTVHMLLFGCNMPSSTGSYWF--CDEGTCTDKAN----ILYAWARNAPPTRLPKGVGFR 157
VHHM +F C S + CD D+ N +L AWA A P+ G
ALVHHMEVFQCTNESEAFPMFNGPCDSKMKPDLNLYCRHVLAAWALGAKAFYYPEEAGVP 136

VGGETGSKYFVLQVHYGDISAFRDNHKDCSGVSVHLTRVPQPLIAGMYLMMSVDT--VI 214
+G S++ L+VHY + + +D SG+ +H T +P AG+ + V T I
LGSSGSSRFLRLLEVHYHNPRNIQ-GRRDSSGIRLHYTASLRPNEAGIMELGLVYTPLMAI 195

PPGEKVVNADISQCQYKMYPM-----HVFAYRVHTHHLGKVVSGYRVRNGQWT-LIGRQ 266
PP E C + M +FA ++HTH G+ V R+GQ ++ R
PPQETTFVLTGYCTDRCTQMALPKSGIRIFASQLHTLTLGRKVVITVLARDGQQREVVNRD 255

NPQLP--QAFYYPVEHPVDVTFGDILAARCVFTGEGRTEATHIGGTSSDEMKNLYIMYYME 324
N P Q +++ V V GD+L C + E RT AT G +EMC Y+ YY +
NHYSHPHQEIRMLKNAVTVHQGDVLTITSCTYNTENRTMATVGGFGILEEMCVNYVHYYPK 315

AKYAL 329
+ L
TELEL 320

```

Figure 3- Compared protein sequences of rat PHM and DBM using BlastP. There is 29% identity and 41% positives.

Considerably less is known about the PAL reaction. Model studies indicate that carbinolamide dealkylation is base-catalyzed (Bundgaard 1991). These data suggest that an enzymatic base abstracts the hydroxyl proton to facilitate conversion to the amide and glyoxylate. Another possibility is that a zinc-based hydroxyl is the enzymatic base; thus, accounting for the zinc dependence of the PAL reaction (Bell 1997).

Using a set of glycine-extended peptides of the form N-dansyl-(Gly)₄-X-Gly, Tamburini et al. (1990) demonstrated that PAM could produce peptides terminating all 20 amino acid amides. The penultimate amino acid does have an effect on the kinetic constants for α -amidation. The V_{MAX}/K_M value obtained for N-dansyl-(Gly)₄-Phe-Gly was 1140-fold higher than that obtained for N-dansyl-(Gly)₄-Glu-Gly. The glycine-extended peptides with a sulfur-containing or hydrophobic amino acid in the penultimate

position exhibited the highest V_{MAX}/K_M values (Table 1). This result was critical in our development of novel sulfur-containing hippurate analogs as PAM inhibitors.

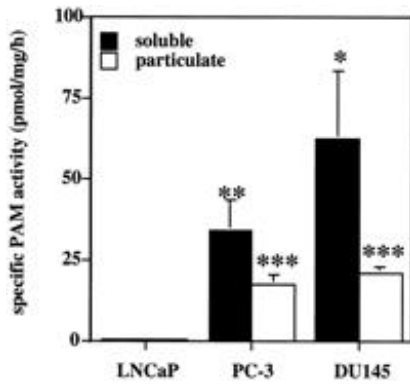
X	K_M (μM)	V_{MAX} (nmol/min/mg)	Relative V_{MAX}/K_M	X	K_M (mM)	V_{MAX} (nmol/min/mg)	Relative V_{MAX}/K_M
Phe	4	50	1140	Ala	46	6	12
Tyr	5	40	730	Asn	83	7	7.6
Met	7	23	300	Arg	200	15	6.8
Ile	20	55	250	Gln	308	17	5.0
Trp	58	58	91	Ser	196	9	4.2
Val	49	48	89	Pro	618	22	3.3
Cys	11	10	83	Lys	206	4	1.7
Leu	54	22	37	Glu	449	5	1.0
His	41	10	22	Gly	-	-	<0.4
Ala	334	50	14	Asp	-	-	-

Table 1- Kinetic parameter for N-dansyl-(Gly)₄-X-Gly amidation

Replacement of the C-terminal glycine with any other D- or L-amino acid, with the exception of D-alanine, did not support PAM catalysis. D-Alanine-extended peptides are relatively poor PAM substrates, exhibiting V_{MAX}/K_M values that are ~0.1% of that obtained for the corresponding glycine-extended peptides. Based on this finding, hippurate and hippurate analogs were used as a lead compounds for developing inhibitors for PAM.

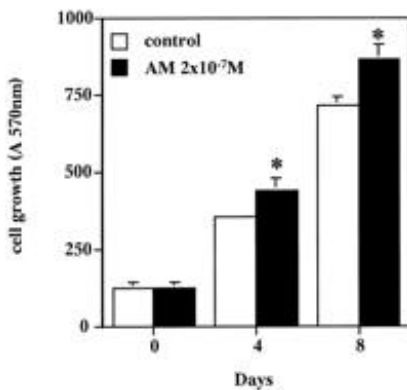
The role of PAM in prostate cancer

Prostate cancer is the second leading cause of cancer death in males today. The probability that a man will contract prostate cancer in his lifetime is reaching 100% (Parker 1996). There are two basic types of prostate cancer: androgen-dependent and androgen-independent (Bonkhoff 1993). Androgen-dependent prostate cancer cells have



Graph 1- PAM activity in androgen-dependent (LNCaP) and androgen-independent (PC-3 and DU 145) prostate cancer cell lines.

many androgen receptors. When deprived of androgen, these cells die. Androgen-independent cells do not have these receptors and do not rely on androgen to proliferate (Rocchi 2001). A common androgen-dependent cell line is LNCaP, and common androgen-independent cell lines are PC-3 and DU 145. Androgen-dependent forms of cancer can be effectively treated by therapeutic hormone deprivation (Kyprianou 1990), but in most cases where androgen-dependent prostate cancer has been suppressed, it reemerges as an androgen-independent form. The pathway for this change is not known, but it is thought that PAM has a role in the proliferation of the newly formed androgen-independent cancer. In androgen-independent strains of prostate cancer, there is a 3-fold greater amount of PAM mRNA. There are also elevated PAM protein levels (Graph 1).



Graph 2- Effect of AM on cell growth of DU 145 prostate cancer cells.

The specific activity of the PAM found in the androgen-independent cell lines is also higher.

Adrenomedullin (AM), a growth-stimulating α -amidating peptide, is produced by androgen-independent prostate tumors (Rocchi 2001). AM is only active in its amidated form. Graph 2 shows the growth rates of DU-145 cells that have been treated with AM. There is a significant increase in cell growth when AM is added. AM does not affect androgen-dependent cells. It is thought that the amount of AM that can be used in these cell lines are at their maximum, thus adding more peptide does not affect these cells (Rocchi 2001).

N-(4-hydroxyphenyl) retinamide (4-HPR) is a known inhibitor of DU-145

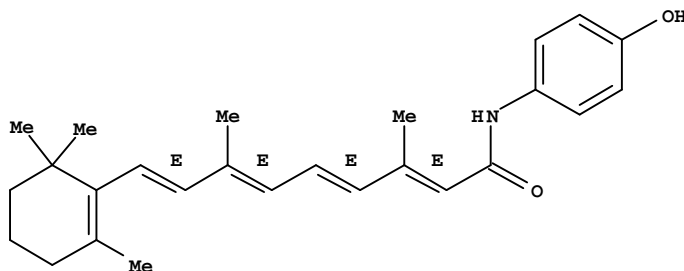
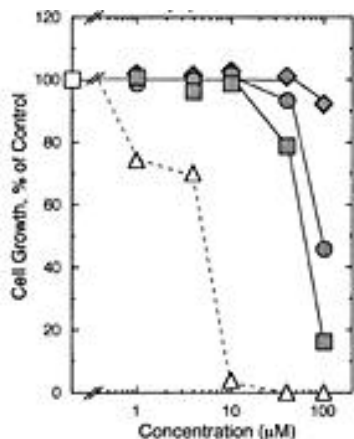


Figure 4- Structure of 4-HPR.

cells (Figure 4). It is thought that 4-HRP undergoes an oxidative pathway that generates reactive oxygen species. These oxygen species are extremely dangerous to cells, since they interrupt pathways by inactivating enzymes. The aminophenol ring and long alkyl chain are key functional groups for drug-cell contact (Takahashi 2002). Aminophenols such as *p*-methylaminophenol (*p*-MAP), 4-aminophenol (4-AP), and *p*-aminoacetophenol (*p*-AAP) have also been shown to stop cell growth. Graph 3 shows the effect of 4-HPR and several aminophenols on the growth of DU 145 cells.



Graph 3- Effects of 4-HPR on DU 145 prostate cancer cell growth. Cells were grown with compound for 72 hours before counting. The clear squares represent control cells, the clear triangles represent 4-HPR, the solid squares represent *p*-MAP, the solid circles represent 4-AP, and the solid diamonds represent *p*-AAP.

Conclusion

Around 50% of all mammalian hormones have the C-terminal á-amidated structure that PAM produces. PAM plays a critical role in the emergence of androgen-independent forms of prostate cancer. The experiments in the following chapters use substrate-based inhibitors targeted for PAM. The kinetic constants were experimentally detected and the most potent compounds were tested on prostate cancer cells to determine if they would halt DU-145 cell proliferation.

Chapter Two

Substrate-Based Inhibitors for PAM

INTRODUCTION

Inhibitors are substances that lower the rate of catalysis of an enzyme. Inhibiting enzymes are one of the most common ways that organisms regulate their biological processes. The binding specificity of a substance towards an enzyme can be determined by studying the inhibition (Segel 1976). In many types of cancer, there are mutated enzymes that cause the spread of the disease, thus inhibiting these enzymes is key to halting cancer proliferation.

Enzyme Inhibition

Three types of inhibition have been described that account for the reversible binding of one inhibitor molecule, I, to one enzyme molecule, E (Figure 5). For competitive inhibition, the inhibitor and substrate, S, compete exclusively for E yielding either the catalytically competent ES complex or the catalytically incompetent EI complex (Figure 5a). Non-competitive inhibition involves the binding of I to E and ES to producing both an EI binary complex and an ESI ternary complex. The affinity of I to E and ES is described by two dissociation constants, K_{is} and K_{ii} , respectively (Figure 5b). If K_{is} equals K_{ii} , the inhibition is usually referred to as non-competitive or pure non-competitive inhibition. If K_{is} does not equal K_{ii} , the inhibition is referred to as mixed-

type inhibition. Uncompetitive inhibition is the binding of I only to the ES complex to generate the inactive ESI complex (Figure 5c). Segal (1976) details other inhibition types, usually involving the reversible binding of more than one inhibitor molecule per enzyme molecules. Such modes of inhibition are infrequently encountered.

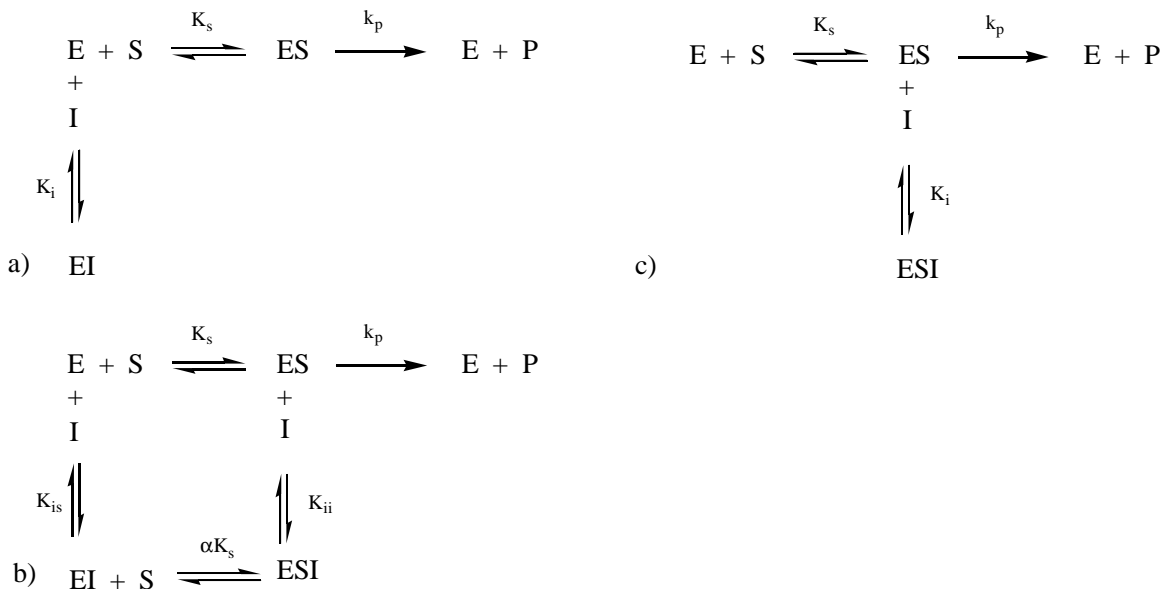


Figure 5- Diagram of a) competitive inhibition, b) non-competitive inhibition, and c) uncompetitive inhibition

Irreversible inhibitors are well known in the enzyme literature and, most often, involve the generation of an inactive enzyme species after the initial formation of the EI complex (Figure 6). The mechanism outlined in Figure 6 can account for mechanism-based, suicide substrates, the chemical modification of active site residues, and slow-binding inhibitors ($k_{\text{inact}} \lll k_p$).



Figure 6- Diagram of irreversible inhibition. For slow-binding inhibition, S and I compete for E (similar to competitive inhibition) and $k_{\text{inact}} \lll k_p$.

N-Benzoylglycine (Hippuric Acid) as Lead Compound

Tamburini et al. (1990) demonstrated that PAM preferred peptide substrates with hydrophobic or sulfur-containing amino acids at the penultimate position. Hippurate is an ideal candidate as an ideal lead compound for the development of small molecules inhibitors of PAM for the following reasons: (a) hippurate is a known PAM substrate, (b) hippurate contains a hydrophobic N-benzoyl group at a position analogous to the penultimate amino acid in C-terminal glycine extended peptides, (c) numerous ring-substituted hippurates and hippurate analogs are commercially available, (d) two sulfur containing hippurate analogs were commercially available, and (e) targeted analogs of hippurate that are not available commercially (with and without sulfur) are relatively straightforward to synthesize.

Given these considerations, we have prepared and evaluated a library of substituted hippurates and hippurate analogs as substrates and inhibitors. The inhibitors with the highest affinity for PAM (lowest values of K_{is} and K_{ii}) were then tested for anti-proliferative behavior vs. prostate cancer cells in culture (Chapter 3).

Methods to Assay for PAM Activity

PAM converts C-terminal glycine-extended peptides to α -amidated peptides and glyoxylate in a reaction that consumes O_2 and reductant (Figure 1). Thus, PAM activity can be measured by assaying for (a) the consumption of O_2 , (b) the consumption of reductant, (c) the production of glyoxylate, and (d) the production of the α -amidated peptide. These different assay methods have advantages and disadvantages and all have been appropriately applied in the study of PAM. The two assay methods employed to

generate the data contained within this thesis were to measure PAM-dependent conversion of N-dansyl-Tyr-Val-Gly to N-dansyl-Tyr-Val-NH₂ by HPLC and to measure the PAM-dependent consumption of O₂ in the presence of an oxidizable substrate.

The PAM-dependent conversion of N-dansyl-Tyr-Val-Gly to N-dansyl-Tyr-Val-NH₂ has been extensively used in the Merkler laboratory (Merkler 1999). This assay is sensitive, requiring relatively small amounts of enzyme and N-dansyl-Tyr-Val-Gly, and can be carried in volumes $\ll 1.0$ ml, particularly important if the small amounts of inhibitor are available*. However, this method is laborious, provides only a discontinuous measure of [product] formed per unit time, and requires the availability of an HPLC equipped with an autosampler, and an inline flow-through fluorescence detector. The development of new HPLC separation methods and syntheses of substrate and product standards are necessary to extend this assay method to other N-dansylated (or otherwise fluorescently-labeled) PAM substrates.

The PAM-dependent consumption of O₂ has also been extensively employed in the Merkler laboratory (Merkler 1999). This method requires only an O₂ electrode, provides a continuous measure of [substrate] consumed per unit time, and is generally useful for any oxidizable substrate. Unfortunately, this assay is less sensitive than assaying for N-dansyl-Tyr-Val-NH₂ production and requires considerable more PAM and substrate. Furthermore, this system has an inherent background rate of O₂ consumption

*Non-fluorescent substrates that compete with N-dansyl-Tyr-Val-Gly for the PAM active site behave as competitive inhibitors (Spector 1981). The K_{is} values obtained using non-fluorescent substrates equal the K_M . The PAM-dependent conversion of N-dansyl-Tyr-Val-Gly to N-dansyl-Tyr-Val-NH₂ is useful to determine K_M values for non-fluorescent substrates of limited availability or those that exhibit low V_{MAX} values.

(from the O₂ electrode and the presence of reductant and Cu(II) ions in the assay buffer) that renders this method difficult to use with substrates of with low V_{MAX} values.

EXPERIMENTAL PROCEDURES

Materials

MES buffer, N-dansyl-Try-Val-Gly, hippuric acid and S-(thiobenzoyl)thioglycolic acid were from Sigma, sodium chloride, ethanol, Triton X-100, HEPES buffer, acetonitrile, sodium acetate, sodium hydroxide, and trifluoroacetic acid were from Fisher Scientific, sodium ascorbic acid was from Research Organics, copper nitrate and isopropanol were from Acros, and catalase was from Worthington Biochemical Corporation. N-Acetylglycine was from T.C.I. Oxygen monitor and electrodes were from Yellow Spring Instrument. Signal amplifier was from Oriel and assembled by Dr. R. Larsen (University of South Florida). N-Phenylhydantoic acid was from Maybridge. (D,L)-Thiorphan was from BACHEM. 4-Ethylhippuric acid, N-(phenylthiopropionyl)glycine, 4-propionylhippuric acid, N-(6-phenylhexanoyl)glycine, N-(8-phenyloctanoyl)glycine, S-(4-methylthiobenzoyl)thioglycolic acid, S-(4-methylthiobenzoyl)thioglycolic acid ethyl ester, S-(phenylthioacetyl)thioglycolic acid, S-(N-phenylthiocarbamoyl)thioglycolic acid, S-(N-phenylthiocarbamoyl)-3-mercaptopropionic acid, N-glycolic acid phenyl urethane, lauroyl-sulfanyl-acetic acid and S-(3-phenylthiopropionyl)thioglycolic acid were from Dr. T. C. Owen (University of South Florida). (Phenylthio)acetic acid and (2-nitrophenylthio)acetic acid were from Dr. J. Vederas (University of Alberta). N-(Phenylthioacetyl)alanine and 4-cyano-4-methyl-4-

thiobenzoyl-sulfanyl-butyric acid were from Dr. A. Lowe (University of Southern Mississippi). HyperChem 7.5 was from Hypercube Inc.

High-performance liquid chromatography

N-Dansyl-Try-Val-Gly and N-dansyl-Try-Val-NH₂ were separated using a Hewlett Packard 1100 Series liquid chromatograph equipped with a quaternary solvent delivery system, vacuum degasser, temperature controlled column compartment, and an auto injector. A Keystone Scientific Operations Thermo Hypersil reverse-phase C₁₈ column (100 mm x 4.6 mm, 5 μm particles, 120 Å pore) fitted with a Phenomenex C₁₈ Security Guard column was used for the separation. A Gilson Model 121 fluorometer and a Hewlett Packard 3392A integrator monitored separations. Hewlett Packard ChemStation controlled the 1100 Series liquid chromatograph.

Bifunctional peptidylglycine α-amidating monooxygenase

Chinese hamster ovary cells that secrete recombinant type A rat medullary thyroid carcinoma PAM into the culture media (Bertelsen, 1990) were grown in a Cellco Cellmax-100 hollow fiber bioreactor (Matthews, 1994). The bifunctional enzyme was purified as described by Miller et al. (1992) except that the final gel filtration step (Superdex-200) was done using 50 mM Tris pH 8.0 and 100 mM NaCl. The amidation of N-dansyl-Tyr-Val-Gly to N-dansyl-Tyr-Val-NH₂ (Jones 1988) and UV detection at 280 nm were used throughout the enzyme purification to screen column fractions.

HPLC separation of dansylated compounds

N-Dansyl-Try-Val-Gly and N-dansyl-Try-Val-NH₂ were separated on a reverse-phase C₁₈ column (100 mm x 4.6 mm, 5 µm particles, 120 Å pore). The mobile phase for the separation consisted of 100 mM sodium acetate, 55% deionized water and 45% acetonitrile. The mobile phase was delivered at a flow rate of 1.2 ml/min. The injection volume was 10 µl. The retention times of the N-dansyl-Try-Val-Gly and Dansyl-Try-Val-NH₂ were 1.3 and 2.35 minutes.

Determination of initial rates of N-dansyl-Try-Val-NH₂ production as fixed N-dansyl-Try-Val-Gly concentration as a function of inhibitor concentration (Dixon analysis)

Reactions at 37 °C were initiated by the addition of PAM (0.05-0.09 µg) into 500 µl of 100 mM MES/NaOH pH 6.0, 30 mM NaCl, 1.0% (v/v) ethanol, 0.001 % (v/v) Triton X-100, 10 µg/ml bovine catalase, 1.0 µM Cu (NO₃)₂, 5.0 mM sodium ascorbate, inhibitors (1.0-2000 µM) and 8 µM N-dansyl-Try-Val-Gly. Aliquots of 50 µl were taken at 5, 10, 15, 20, and 25 minutes. The reaction aliquot was quenched with 10 µl of 6 % (v/v) trifluoroacetic acid in a HPLC microvial to terminate the PAM reaction. The aliquots were assayed for N-dansyl-Try-Val-Gly and dansyl-Try-Val-NH₂ on a reverse-phase C₁₈ column (100 mm x 4.6 mm, 5 µm particles, 120 Å pore). The mobile phase for the separation consisted of 100 mM sodium acetate, 55% deionized water and 45% acetonitrile.

Determination of K_M and V_{MAX} values for N-dansyl-Tyr-Val-Gly as a function of inhibitor concentration

Reactions at 37 °C were initiated by the addition of PAM (0.02–0.03 µg) into 500 µl of 100 mM MES/NaOH pH 6.0, 30 mM NaCl, 1.0% (v/v) ethanol, 0.001 % (v/v) Triton X-100, 10 µg/ml bovine catalase, 1.0 µM Cu (NO₃)₂, 5.0 mM sodium ascorbate, N-dansyl-Tyr-Val-Gly (1.25–12.5 µM), and inhibitor (20–800 µM). Aliquots of 50 µl were taken at 5, 10, 15, 20, and 25 minutes. The reaction aliquot was quenched with 10 µl of 6 % (v/v) trifluoroacetic acid in a HPLC microvial to terminate the PAM reaction. The aliquots were assayed for N-dansyl-Tyr-Val-Gly and N-dansyl-Tyr-Val-NH₂ on a reverse-phase C₁₈ column (100 mm x 4.6 mm, 5 µm particles, 120 Å pore). The mobile phase for the separation consisted of 100 mM sodium acetate, 55% deionized water and 45% acetonitrile.

Determination of initial rates by oxygen consumption

In order to determine kinetic constants (K_M and V_{MAX}), reactions at 37 °C were initiated by the addition of PAM (0.03–0.06 µg) into 2700 µl of 100 mM MES/NaOH pH 6.0, 30 mM NaCl, 1.0% (v/v) ethanol, 0.001 % (v/v) Triton X-100, 10 µg/ml bovine catalase, 1.0 µM Cu (NO₃)₂, 5.0 mM sodium ascorbate, and substrate (3.0–2500 µM). V_{MAX} values were normalized to controls ran at 11 mM N-acetylglycine. Rates were monitored, recorded, and analyzed in Microsoft Excel.

In order to determine the K_i values (Dixon analysis), reactions at 37 °C were initiated by the addition of PAM (0.03–0.06 µg) into 2700 µl of 100 mM MES/NaOH pH

6.0, 30 mM NaCl, 1.0% (v/v) ethanol, 0.001 % (v/v) Triton X-100, 10 µg/ml bovine catalase, 1.0 µM Cu (NO₃)₂, 5.0 mM sodium ascorbate, 9 mM N-acetylglycine, and inhibitor (1.0-200 µM). Rates were monitored, recorded, and analyzed in Microsoft Excel.

Copper Chelating Experiment

Reactions at 37 °C were initiated by the addition of 0.05 µg PAM into 500 µl of 100 mM MES/NaOH pH 6.0, 30 mM NaCl, 1.0% (v/v) ethanol, 0.001 % (v/v) Triton X-100, 10 µg/ml bovine catalase, 1.0 µM Cu (NO₃)₂, and 5.0 mM sodium ascorbate. Three dansyl Tyr-Val-Gly concentrations of 4µM, 10µM, and 20µM were tested. S-(4-methylthiobenzoyl)thioglycolic acid was tested at 12 µM and EDTA was tested at 30 µM. Both compounds were tested at the three different N-dansyl Tyr-Val-Gly concentrations. Aliquots of 50 µl were taken at 5, 10, 15, 20, and 25 minutes. The reaction aliquot was quenched with 10 µl of 6 % (v/v) trifluoroacetic acid in a HPLC microvial to terminate the PAM reaction. The aliquots were assayed for N-dansyl-Tyr-Val-Gly and N-dansyl-Tyr-Val-NH₂ on a reverse-phase C₁₈ column (100 mm x 4.6 mm, 5 µm particles, 120 Å pore). The mobile phase for the separation consisted of 100 mM sodium acetate, 55% deionized water and 45% acetonitrile.

Molecular Modeling

HyperChem 7.5 was used for performing molecular modeling. Substrates and inhibitors were calculated to their lowest energy states using Amber 99. The compounds were then inserted into the active site of PHM in both the phenyl ring in (substrate-like)

and the phenyl ring out confirmations. The lowest energy conformation was determined by the method of Polak-Ribiere. The energies were compared to the energy of the unbound reduced enzyme to determine the stability of the enzyme-inhibitor complex.

RESULTS AND DISCUSSION

PAM substrates and inhibitors

Results from this study (Table 2) suggest that compounds with sulfanyl type groups, such as S-(phenylthioacetyl)thioglycolic acid and S-(N-phenylthiocarbamoyl)-3-mercaptopropionic acid, appear to bind more tightly than compounds with hydrogen or oxygen. (Phenylthio)acetic acid does not have a sulfanyl group and has a much higher K_i . Substrates with oxygen have a much higher K_M than those with sulfanyls. This trend can be seen when comparing the K_M of N-(phenylthiopropionyl)glycine to N-(6-phenylhexanoyl)glycine (Table 3). Since sulfur has a higher electron density than oxygen, it is possible that this atom interacts with the two coppers in the active site. In addition, since redox chemistry is necessary for the reaction to proceed and altering the coordinating sphere of copper ions could dramatically affect the reduction potentials, the sulfur atoms could interfere with electron transfer within the enzyme.

Another class of compounds that exhibit tight binding contains other functional groups on the benzene ring. For example, methyl groups in the para position exhibit tight binding. S-(4-Methylthiobenzoyl)thioglycolic acid has this moiety and has the low K_i of 3.5 μ M. 4-Ethylhippuric acid and 4-propionylhippuric acid are two substrates with

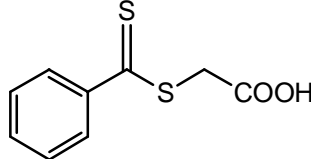
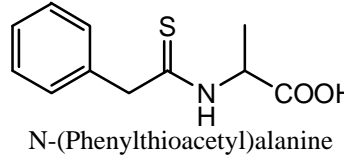
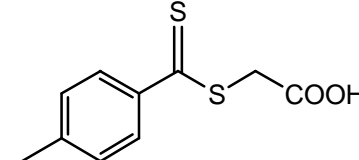
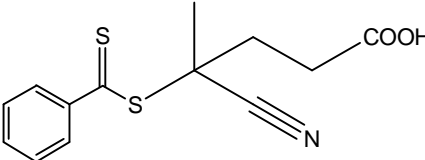
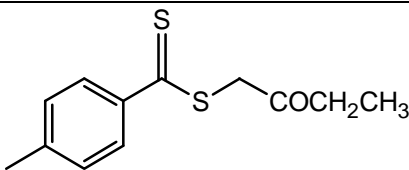
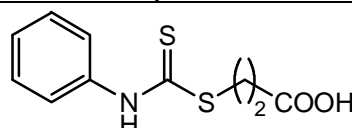
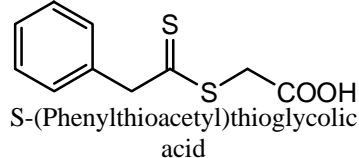
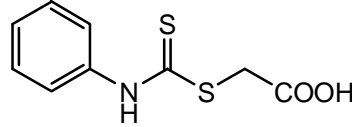
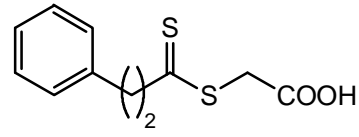
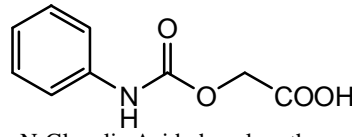
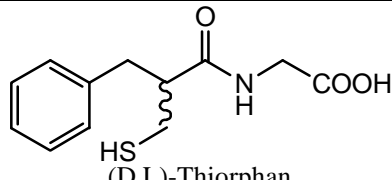
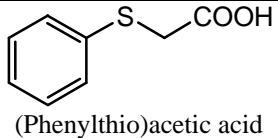
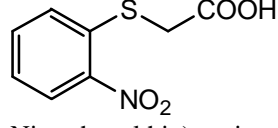
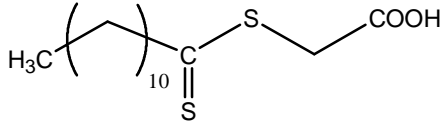
Inhibitor	$K_{i,app}$ (μM)	Inhibitor	$K_{i,app}$ (μM)
 S-(Thiobenzoyl)thioglycolic acid	39 ± 5.2	 N-(Phenylthioacetyl)alanine	3.6 ± 0.4
 S-(4-Methylthiobenzoyl)thioglycolic acid	3.5 ± 0.39	 4-Cyano-4-methyl-4-thiobenzoyl-sulfanylbutyric acid	20 ± 5.8
 S-(4-Methylthiobenzoyl)thioglycolic acid ethyl ester	110 ± 12	 S-(N-Phenylthiocarbamoyl)-3-mercaptopropionic acid	3.3 ± 0.88
 S-(Phenylthioacetyl)thioglycolic acid	7.9 ± 2.8	 S-(N-Phenylthiocarbamoyl)thioglycolic acid	11 ± 1.9
 S-(3-Phenylthiopropionyl)thioglycolic acid	9.4 ± 0.8	 N-Glycolic Acid phenyl urethane	54 ± 4.0
 (D,L)-Thiorphan	22 ± 2.6	 (Phenylthio)acetic acid	380 ± 36
 (2-Nitrophenylthio)acetic acid	29 ± 3.4	 S-(Thiolauroyl)thioglycolate	0.54 ± 0.045

Table 2- Summary of inhibitors examined and corresponding inhibition constants. Inhibition constants were calculated by Dixon analysis.

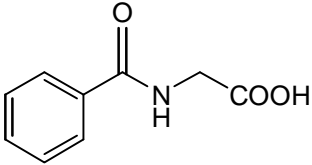
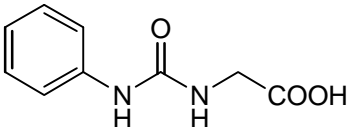
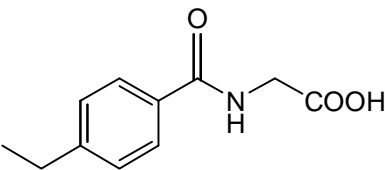
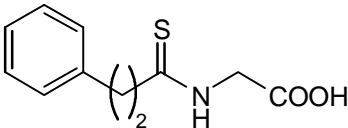
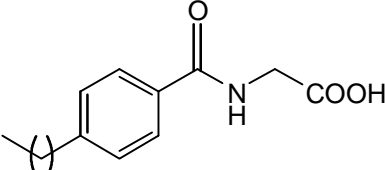
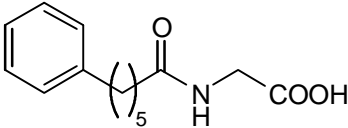
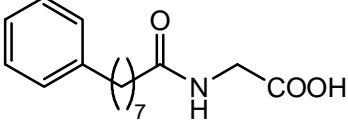
Substrate	$K_{M,app}$ (μM)	$V_{MAX,app}$ ($\mu\text{moles/min}$ /mg)	$(V/K)_{app}$ ($\text{M}^{-1}\text{s}^{-1}$)	Relative ($V/K)_{app}$
 Hippuric acid	1300 ± 36	$6.5 \pm .063$	6.2×10^3	1.0
 N-Phenylhydantoic acid	350 ± 70	7.6 ± 0.65	2.7×10^4	4.4
 4-Ethylhippuric acid	1162.1 ± 166.45	2.9 ± 0.2	2.8×10^3	0.45
 N-(Phenylthiopropionyl)glycine	38 ± 15	1.3 ± 0.11	4.3×10^4	6.9
 4-Propionylhippuric Acid	1207.3 ± 157.64	4.1 ± 0.3	4.1×10^3	0.66
 N-(6-Phenylhexanoyl)glycine	96 ± 14	8.2 ± 0.53	1.1×10^5	17
 N-(8-Phenyloctanoyl)glycine	104.84 ± 9.3273	6.4 ± 0.2	1.2×10^5	19

Table 3- Summary of substrates examined and corresponding kinetic constants. Kinetic constants were calculated using Michaelis-Menton calculations.

extended hydrocarbon chains in the para position. Interestingly this did not seem to affect the binding affinity. In addition, functional groups at the ortho position dramatically increase the binding affinity. (2-Nitrophenylthio)acetic acid has a 12-fold tighter binding affinity to (phenylthio)acetic acid.

The length of the hydrocarbon chain also affects the binding affinity of the inhibitors. S-(Thiobenzoyl)thioglycolic acid, S-(phenylthioacetyl)thioglycolic acid, and S-(3-phenylthiopropionyl)thioglycolic acid have the same structure with the exception of the hydrocarbon chain before the sulfanyl group. The trend in binding affinity shows that in this group of compounds, the ideal length for inhibition is two carbon groups prior to the sulfanyl. The substrates N-(6-phenylhexanoyl)glycine and N-(8-phenyloctanoyl)glycine show that PAM prefers a lengthy hydrocarbon chain since their K_M are 13-fold lower than hippurate.

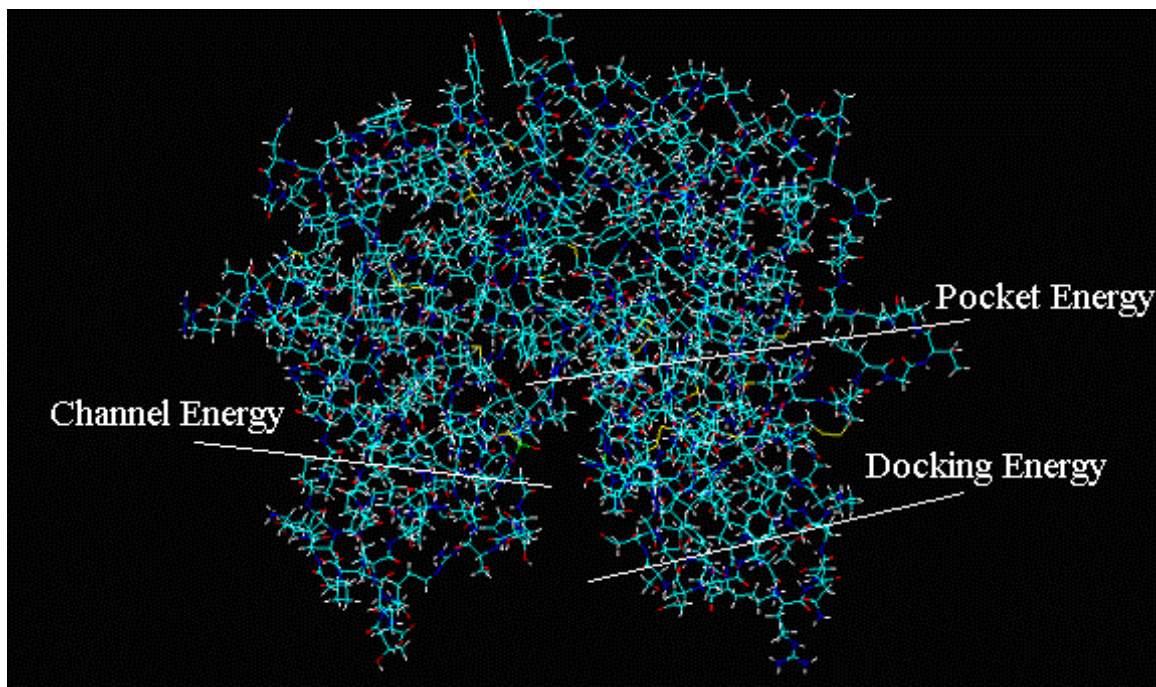


Figure 7- Different energies that can be predicted by molecular modeling.

Molecular modeling was performed to understand the relationship between K_i and binding energies of the compounds to better understand the structure activity of the PAM. There are three types of energies to consider when determining the total free energy of a

$$\text{a.) } \Delta G = \Delta G_{\text{docking}} + \Delta G_{\text{channel}} + \Delta G_{\text{pocket}}$$

$$\text{b.) } \Delta G_{\text{pocket}} = \Delta H_{\text{pocket}} - T\Delta S_{\text{pocket}}$$

Figure 8- a.) The formula to calculate the total free energy for the complete docking of a compound into the active site of PHM. b.) The formula for calculating the free energy for the pocket energy. Hyper Chem 7.5 calculates the pocket enthalpy.

compound in the active site of PHM (Figure 7). The first of these energies is the docking energy. This is the energy for the compound to enter the active site. The second is the channel energy, which is the energy of the compound to move through the active site channel to get to the binding site. The last is the pocket energy once inside the binding pocket (Figure 8a). The program used in this study, Hyperchem 7.5, is capable of calculating the channel enthalpies and the pocket enthalpies, which can be used to calculate the channel and pocket energies (Figure 8b). A more sophisticated software program is required to calculate the docking enthalpies and actually proposing a specific path that the compound travels from entering the channel to binding into the pocket of the enzyme. For the preliminary studies only the pocket enthalpies were calculated for known substrates and inhibitors of PAM.

The results from the molecular modeling can be seen in Table 4. The enthalpy of the reduced form of PHM without a substrate or inhibitor in the binding pocket was calculated. The enthalpies of the substrates and inhibitors were subtracted from the unbound enthalpy to give the pocket enthalpy. The stability of a compound in the

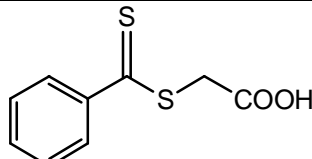
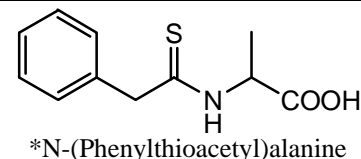
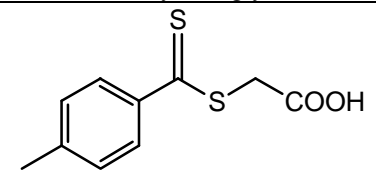
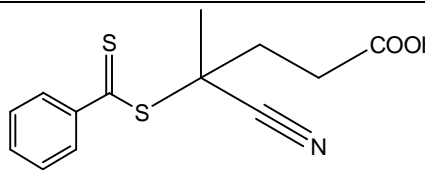
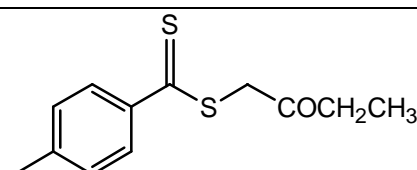
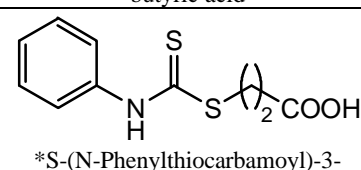
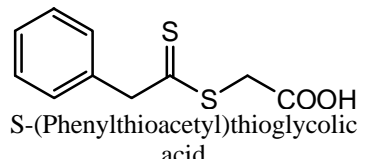
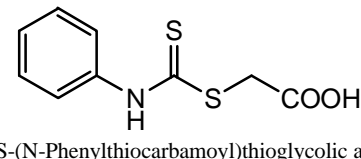
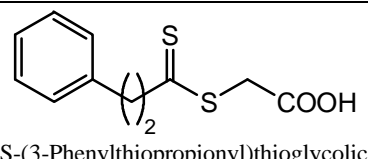
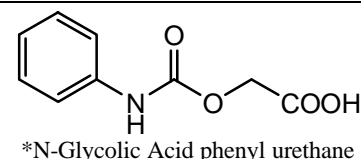
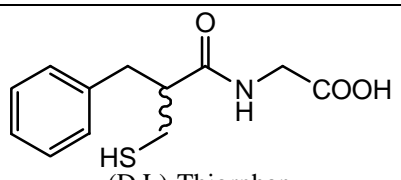
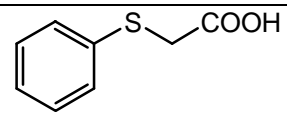
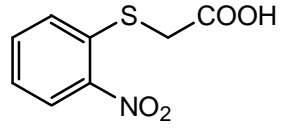
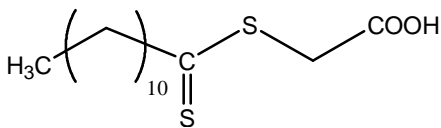
Inhibitor	Bond Energy (kJ/mol)	Inhibitor	Bond Energy (kJ/mol)
 <p>S-(Thiobenzoyl)thioglycolic acid</p>	-10.88	 <p>*N-(Phenylthioacetyl)alanine</p>	-16.91
 <p>*S-(4-Methylthiobenzoyl)thioglycolic acid</p>	-20.92	 <p>*4-Cyano-4-methyl-4-thiobenzoyl-sulfanylbutyric acid</p>	-18.87
 <p>S-(4-Methylthiobenzoyl)thioglycolic acid ethyl ester</p>	-17.91	 <p>*S-(N-Phenylthiocarbamoyl)-3-mercaptopropionic acid</p>	-16.51
 <p>S-(Phenylthioacetyl)thioglycolic acid</p>	-15.11	 <p>*S-(N-Phenylthiocarbamoyl)thioglycolic acid</p>	-15.13
 <p>S-(3-Phenylthiopropionyl)thioglycolic acid</p>	-21.51	 <p>*N-Glycolic Acid phenyl urethane</p>	-10.81
 <p>(D,L)-Thiorphan</p>	-38.37	 <p>*(Phenylthio)acetic acid</p>	-9.99
 <p>(2-Nitrophenylthio)acetic acid</p>	-11.5	 <p>* S-(Thiolauroyl)thioglycolate</p>	-19.07

Table 4- Summary of pocket enthalpies. The * represents compounds that bind substrate-like.

binding site increases as calculated pocket enthalpy decreases. The substrates and inhibitors were calculated inside the binding site of PHM in two conformations. The phenyl group was placed going into the pocket, which is substrate-like, and placed coming out of the pocket. The inhibitors showed stability in both conformations,

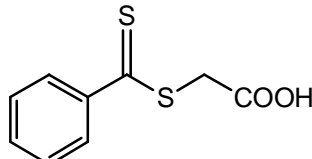
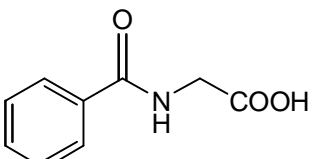
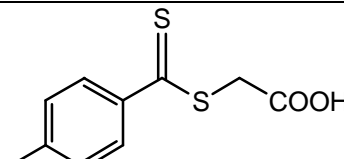
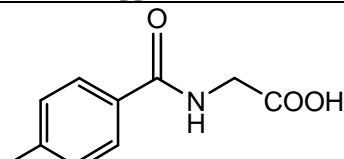
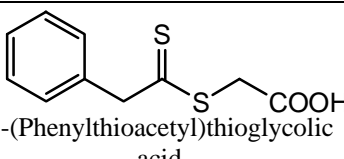
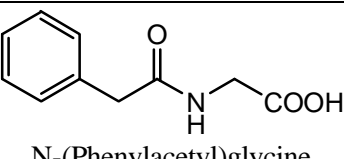
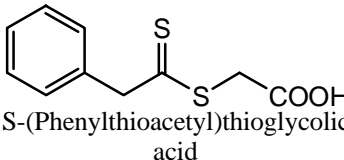
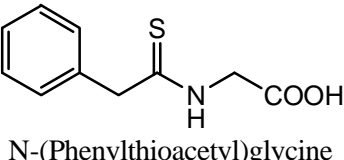
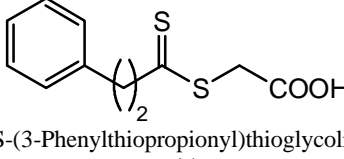
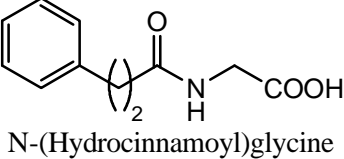
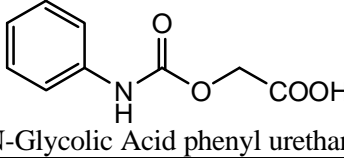
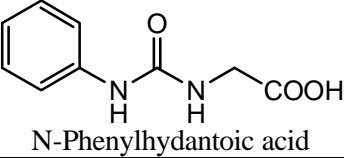
Inhibitor	Bond Energy (kJ/mol)	Substrate	Bond Energy (kJ/mol)
 S-(Thiobenzoyl)thioglycolic acid	-10.88 (39)	 Hippuric acid	-11.00 (1300)
 S-(4-Methylthiobenzoyl)thioglycolic acid	-20.92 (3.5)	 4-Methylhippuric acid	-13.27 (1800)
 S-(Phenylthioacetyl)thioglycolic acid	-15.11 (7.9)	 N-(Phenylacetyl)glycine	-14.95 (150)
 S-(Phenylthioacetyl)thioglycolic acid	-15.11 (7.9)	 N-(Phenylthioacetyl)glycine	-37.30 (24)
 S-(3-Phenylthiopropionyl)thioglycolic acid	-21.51 (9.4)	 N-(Hydrocinnamoyl)glycine	-11.96 (920)
 N-Glycolic Acid phenyl urethane	-10.81 (54)	 N-Phenylhydantoic acid	-12.14 (350)

Table 5- Comparison of inhibitor and substrate pocket enthalpies and binding constants. The number in () represents either K_i for inhibitors or K_M for substrates in μM .

depending on what substituents were on the phenyl ring. All of the substrates showed the preference of the phenyl ring going into the binding pocket.

There is a correlation between pocket enthalpies and the binding constants. As a general trend, if the K_i of an inhibitor is less than $10 \mu\text{M}$, the enthalpy predicted will be < -15 . The active site contains two copper atoms, Cu_H and Cu_M , which cycle through Cu^II and Cu^I redox states during catalysis. The two coppers are non-equivalent, Cu_M being the oxygen-binding site and Cu_H an electron-donor site. All of the compounds gravitated toward Cu_M . This would suggest that there is an important interaction going on with this copper site.

The enthalpies of some substrates and their corresponding inhibitors can be seen in Table 5. The pocket enthalpies of the substrates seem to coincide with their K_M 's, with the exception of 4-methyl hippuric acid. It shows more stability than hippuric acid inside the binding site even though it has a higher K_M . This does not follow the trend of the inhibitors in which the hippuric acid derivative is a much worse inhibitor than the 4-methyl hippuric acid derivative. When the carbonyl is changed to a sulfanyl the compound becomes more stable in the binding pocket.

There are a few compounds where the pocket enthalpies and the binding constants do not seem to correlate. (Phenylthioacetic) acid has a high binding constant, but its pocket enthalpy does not seem to be that much less than other compounds with lower binding constants. This compound may have a low docking enthalpy, so it can get into the channel, but may not bind to the substrate site well. This would effectively block substrates from binding to the enzyme. Based on the pocket enthalpy from 4-cyano-4-methyl-4-thiobenzoyl-sulfanyl-butyric acid, it would be expected that it would be a tight

binding inhibitor, but it does not appear to be. This compound may not bind well to the active site (high docking enthalpy), but if it were able to access the substrate site, the enzyme-inhibitor complex would have a relatively low $K_{\text{dissociation}}$. The same thing could be happening with thiorphan. Another possible reason for the differences in pocket enthalpies and binding constants may be that the compounds are binding to a different site on the enzyme other than the active site. In any case this shows that there is a high probability that there is more than one way a compound binds into the active site of PHM.

When the substrates were tested using the dansyl assay and the oxygen consumption assay, the binding constants were found to be relatively close except for two compounds. 4-Ethylhippuric acid and 4-propionylhippuric acid have roughly a 4-fold difference (Table 4) in K_M . This may be due to an unforeseen PAL inhibition or possible substrate inhibition. This may also indicate that the K_M determined by oxygen

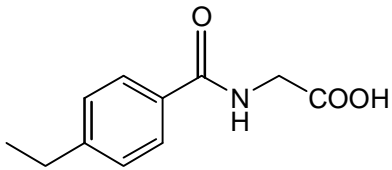
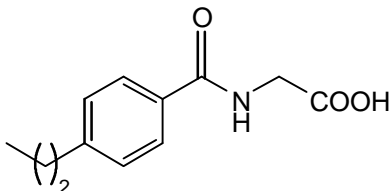
Substrate	$K_{I,\text{app}}$ Dansyl Assay (μM)	$K_{M,\text{app}}$ Oxygen consumption (μM)
 4-Ethylhippuric Acid	370 ± 37	1200 ± 170
 4-Propionylhippuric Acid	350 ± 38	1200 ± 160

Table 6- This is a comparison of K_M value from the oxygen consumption assay and the K_i value from the dansyl assay that show significant differences.

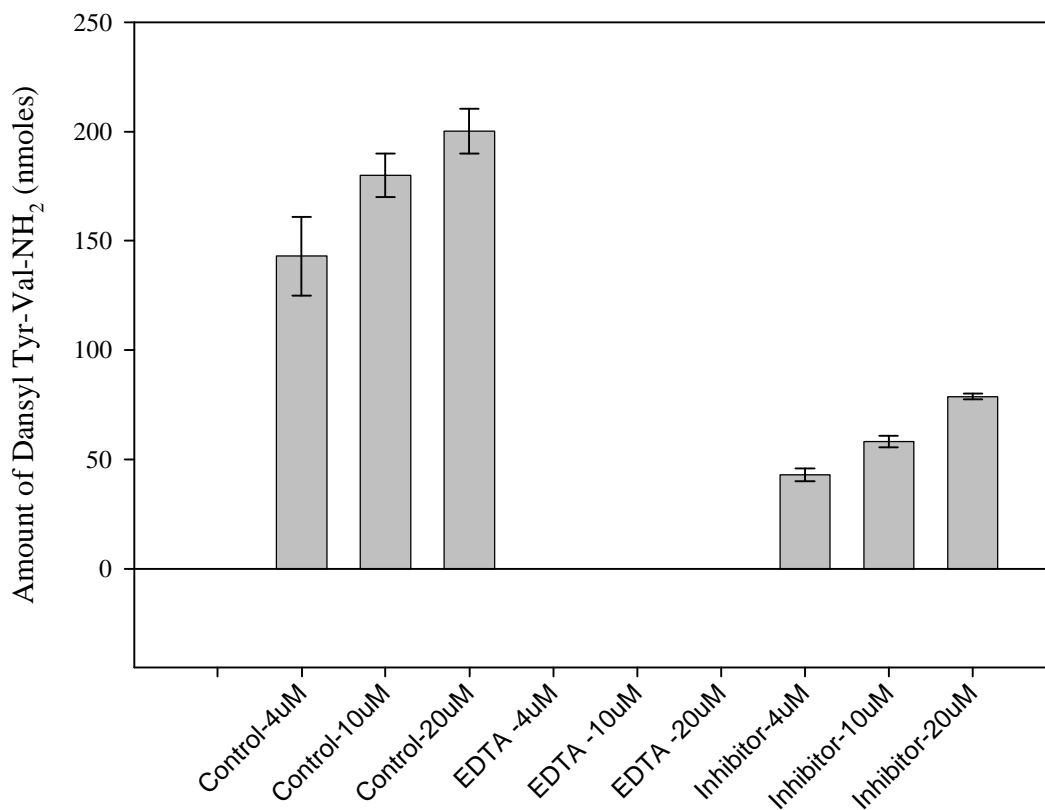
consumption is greater than the true K_d .

Copper chelating experiment

An experiment was performed to determine if the sulfur-containing inhibitors inhibit PAM by competing with substrate for the active site or if they simply depleted copper from the enzyme through chelation. If the inhibitors were depleting the enzyme of copper, the resulting apo-enzyme would be catalytically inactive and could not generate product from substrate at any concentration. On the other hand, if the compounds inhibited the enzyme, increasing the substrate concentration would out compete the inhibitor and product formation would increase as the substrate concentration increased. As seen in Graph 4, the inhibitor, S-(4-methylthiobenzoyl)thioglycolic acid, showed an increase of product formation, as the substrate concentration was increased. To ensure that this result was accurate, the amount of inhibitor used was 3 times the K_i . There was no product formation when EDTA was added to the reaction.

Determination of K_M and V_{MAX} values for N-dansyl-Tyr-Val-Gly as a function of inhibitor concentration

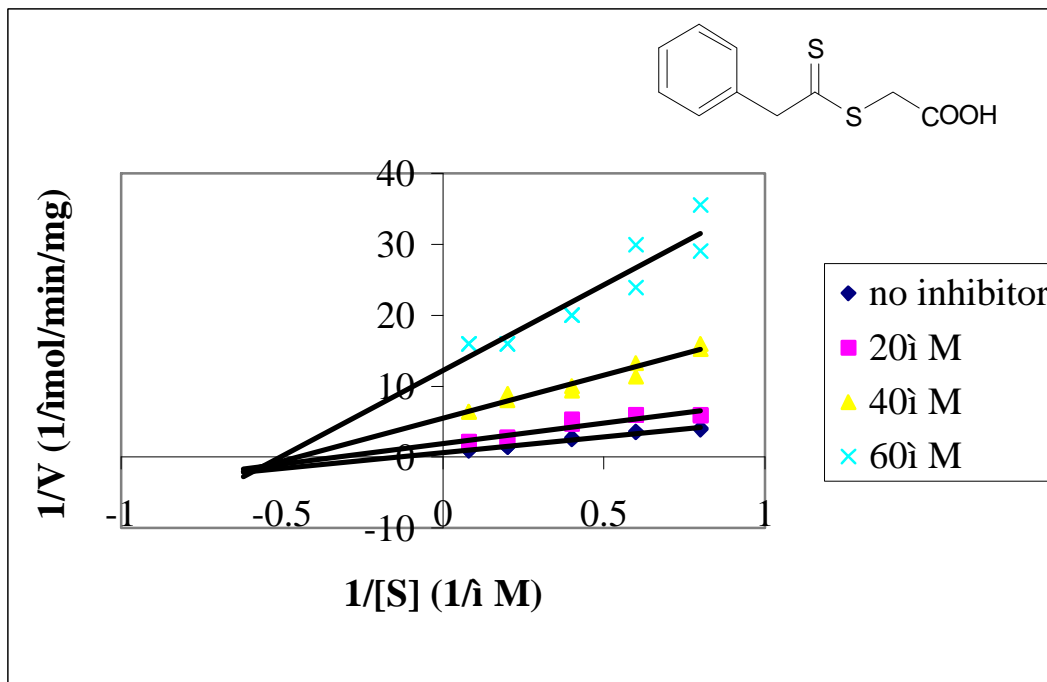
The results from a full inhibition study of S-(3-phenyl thiopropionyl) thioglycolic acid (Graph 5) indicated mixed inhibition, which was contradictory to previous models. The K_{is} calculated was $25 \pm 10 \mu\text{M}$ and the K_{ii} was calculated to be $0.31 \pm 0.18 \mu\text{M}$. The



Graph 4- Plot of product formation vs. substrate concentration in 4, 10, and 20 μ M of EDTA and S-(4-methylthiobenzoyl)thioglycolic acid ($K_i = 3.5 \mu$ M).

K_{is} found in this experiment was similar to the K_i calculated in previous experiments.

The theory was that the inhibitors were competitive. To verify the finding of mixed-type inhibition, a known competitive substrate was tested in the dansyl assay. The results from the experiments with N-octanoyl glycine (Graph 6) showed competitive inhibition with the N-dansyl-Tyr-Val-Gly with a K_{is} of $550 \pm 64 \mu$ M, which is similar to the K_M measured by O_2 consumption ($200 \pm 10 \mu$ M).

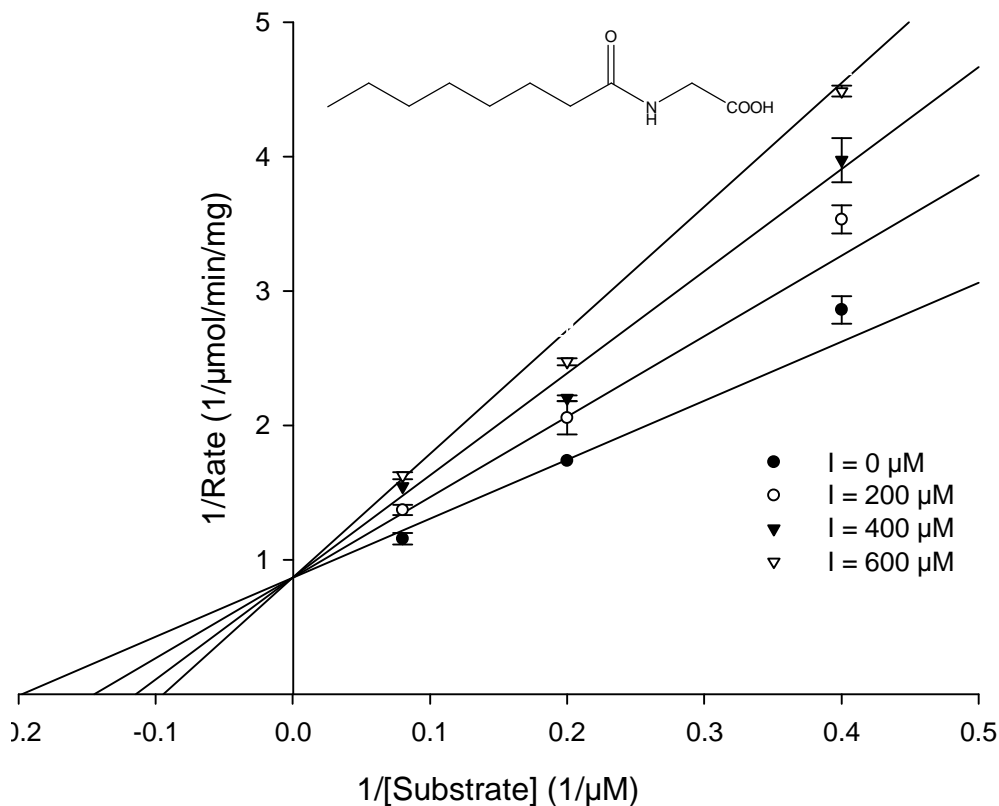


Graph 5- Full kinetic study of S-(3-phenyl thiopropionyl) thioglycolic acid.

Conclusion

The kinetic constants of several substrates and inhibitors of PAM were determined. Several inhibitors were shown to have inhibition constants in the low micromolar range and one, S-(thiolauroyl)thioglycolate exhibited a submicromolar inhibition constant of $0.54 \pm 0.0045 \mu\text{M}$. Through molecular modeling, a preliminary trend in the K_i values was found. Inhibitors with a K_i less than $10 \mu\text{M}$ show a pocket enthalpy of less than -15.0 kJ/mol . Proposed molecules can be placed in the binding site of PHM to predict the K_i . The modeling also shows evidence of more than one binding mode. Some of the inhibitors follow the binding pattern of substrate, and other prefer to be oriented in the reverse position. The full kinetic study of S-(3-phenyl thiopropionyl)

thioglycolic acid supports the idea that some of these inhibitors exhibit more than one



Graph 6- Full kinetic study of N-octanoyl glycine

binding mode to PAM. S-(3-phenyl thiopropionyl)thioglycolic acid is one of the inhibitors that shows a preference for the reverse conformation. Further modeling should be performed on additional compounds to learn more about the structure-activity relationship between binding compounds and PHM. Determination of channel enthalpies and docking enthalpies will also help show the pathway of binding. The inhibitors with the lowest inhibition constant were tested for cancer growth inhibition.

Chapter Three

Prostate Cancer Testing

INTRODUCTION

DU 145 Anti-Proliferation Assays

PAM is suspected to play an important role in androgen-independent prostate cancer proliferation. Two androgen-independent prostate cancer cell lines often used in cancer research are the DU 145 and PC-3 cells. The experiments discussed in this chapter utilize DU 145 androgen-independent cells to probe the effects of PAM inhibitors on cell growth.

Trypan blue stains only dead cells and thus, is used to assay for cell viability. This assay finds wide utilization in many types of cancer research (Lee2001). Another assay used to assay cell viability is dependent upon the production of NADH, a metabolic product of living cells. NADH production drives the reduction of a tetrazolium (MTT, being frequently employed) to an intensely colored formazan (Rocchi 2001).

S-(4-Methylthiobenzoyl)thioglycolic acid and S-(phenylthioacetyl)thioglycolic acid were chosen for this study based on low inhibition constants and stability. S-(*N*-Phenylthiocarbamoyl)thioglycolic acid and S-(*N*-phenylthiocarbamoyl)-3-mercaptopropionic acid exhibit lower inhibition constants, but cyclize at pH values < 10.

S-(*N*-Phenylthiocarbamoyl)thioglycolic acid has a $t_{1/2}$ of 30 minutes and S-(*N*-phenylthiocarbamoyl)-3-mercaptopropionic acid has a $t_{1/2}$ of 8 hours at pH less than 10.

N- (4-Hydroxyphenyl) retinamide (4-HPR) was used as a control. This is a known growth inhibitor of DU 145 cells. The aminophenol ring and the long alkyl chain are two important structures on this compound that are key for drug-cell contact (Takahashi 2002). The target enzyme that 4-HPR inhibits is not known.

EXPERIMENTAL PROCEDURES

Materials

0.05% Trypsin/ 0.53 mM EDTA w/o Ca, Mg, and NaHCO₃, minimum essential medium Eagle (EMEM), and phosphate buffered saline (PBS) were from Cellgro. Trypan blue (0.4% units) was from Life Technologies. Fetal bovine serum (FBS) was obtained from Atlanta Biologicals. Hank's Balanced Salt (HBS) was obtained from ICN Biomedicals. DU 145 prostate cancer cell line was obtained from ATCC. Sodium pyruvate and sodium bicarbonate were obtained from Fisher. Cell culture was carried out in a Nuaire flow hood. Samples were observed under a Nilon TMS phase-contrast microscope.

Cells and cell culture

The DU 145 prostate cancer cells were grown in Eagle's minimum essential medium (EMEM) with Earle's Salts (CaCl₂, KCl, MgSO₄, and Na₂HPO₄) and 2 mM glutamine. The growth media also contained, 1.0 mM sodium pyruvate, 0.1 mM

nonessential amino acids (contains all 20 amino acids), 1.5 g/L sodium bicarbonate, 10% FBS, 10,000 U/ml penicillin, and 10,000 U/ml of streptomycin (Papsidero 1981).

Anti-proliferation assay of S-(4-methylthiobenzoyl)thioglycolic acid

DU 145 cells were grown to 80% confluency in media as described. The cells were then trypsonized, counted, and diluted to give 50,000 cells per well. The cells were allowed to attach to the bottom of the wells for 24 hours. The media was replaced and S-(4-methylthiobenzoyl)thioglycolic acid was added to the media in concentrations of 0.1 mM, 0.5 mM, and 1 mM. S-(4-methylthiobenzoyl)thioglycolic ethyl ester was tested at a concentration of 0.1 mM as a comparison. Cells were then counted at 24, 48, 72, and 96 hours. For each time point, the media was removed the cells and the cells were washed twice with PBS. Trypsin/EDTA was added to detach cells. Media (2 ml) was added to each well, mixed, and removed. A sample from each well was taken out and Trypan blue and HBS were added. The viable and non-viable cells were counted on a hemacytometer. Viable cells appeared clear and non-viable cells appeared blue (Lee 2001).

Anti-proliferation assay of S-(phenylthioacetyl)thioglycolic acid

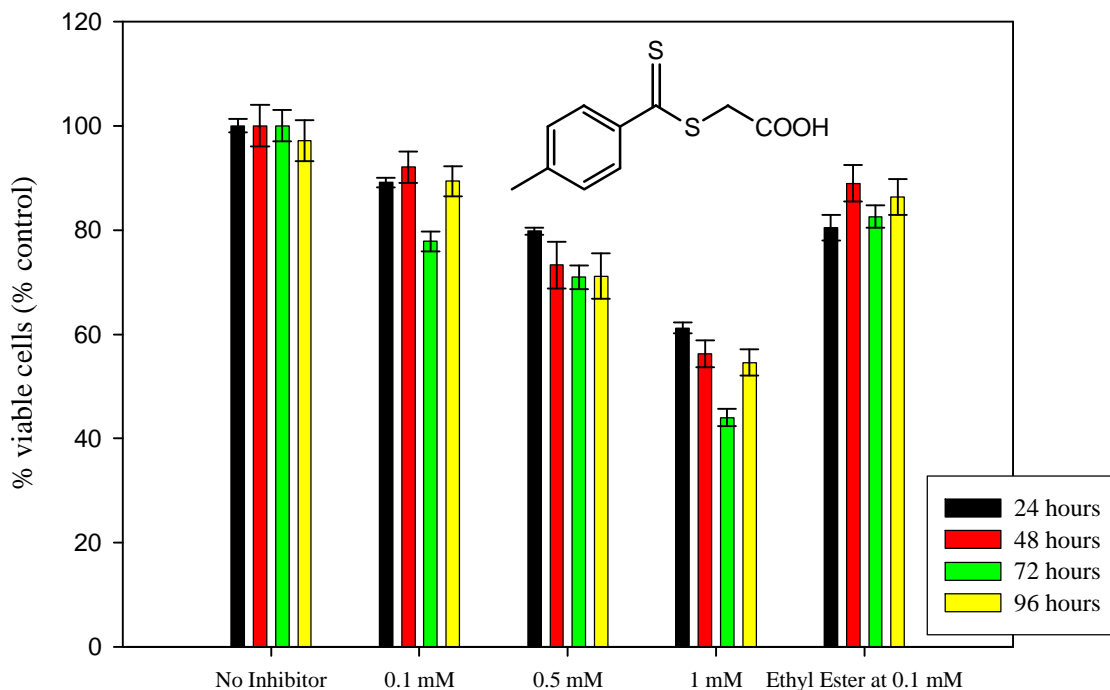
DU 145 cells were grown to 80% confluency as described. Cells were trypsonized, counted, and diluted to give 50,000 cells per well. The cells were allowed to attach to the bottom of the wells for 24 hours. The media was replaced and S-(phenylthioacetyl)thioglycolic acid was added to the media in concentrations of 0.5 mM, 1 mM, and 2 mM. 4-HPR was tested at a concentration of 0.01 mM as a positive control. Cells were then counted at 8, 24, 48, 72, and 96 hours. For each time point, the media

was removed the cells and the cells were washed twice with PBS. Trypsin/EDTA was added to detached cells. Media (2 ml) was added to each well, mixed, and removed. A sample from each well was taken out and Trypan blue and HBS were added. The viable and non-viable cells were counted on a hemacytometer. Viable cells appeared clear and non-viable cells appeared blue (Lee 2001).

RESULTS AND DISCUSSION

Anti-proliferation assay of S-(4-methylthiobenzoyl)thioglycolic acid

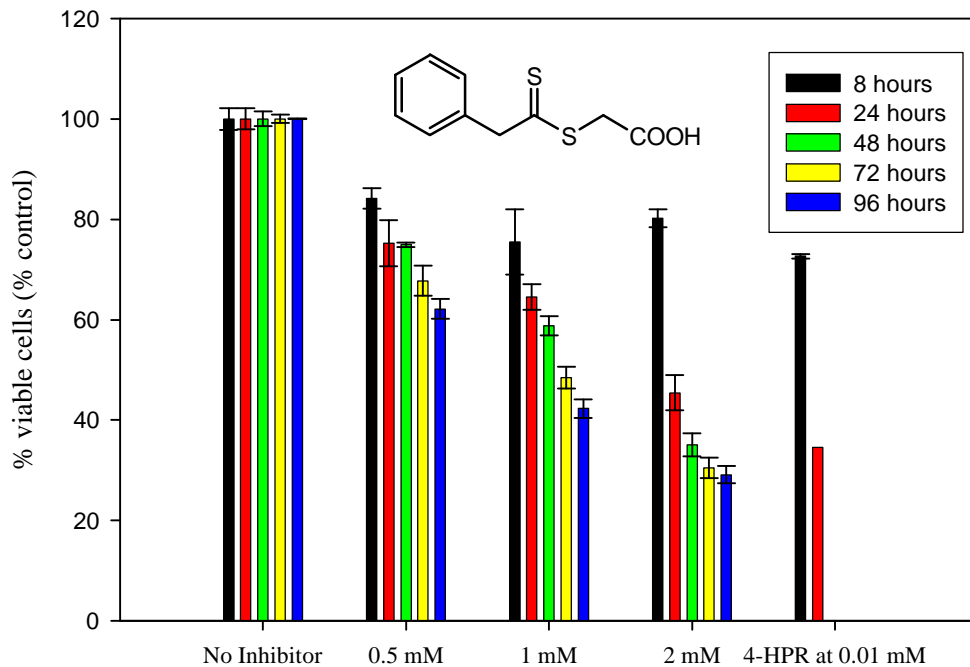
The results of the anti-proliferative assay with S-(4-methylthiobenzoyl)thioglycolic acid can be seen in Graph 7. S-(4-Methylthiobenzoyl)thioglycolic acid does inhibit the growth of androgen-independent prostate cancer, but only at relatively high concentrations (1.0mM). There is only a significant decrease of growth at a concentration of 1 mM for S-(4-methylthiobenzoyl)thioglycolic acid. This concentration is likely to be too high to be of any practical use as an anti-cancer drug. To counter this problem, the ethyl ester of S-(4-methylthiobenzoyl)thioglycolic acid was tested. It was thought that the ethyl ester would make the compound more hydrophobic and would facilitate transport across the cell membrane into the cell. Once inside the cell, an esterase would hydrolyze off the ethyl ester leaving S-(4-methylthiobenzoyl)thioglycolic acid. As the results show, the ethyl ester was no more effective than the free acid as an anti-proliferative agent. Since the K_i of the ethyl ester is ~30-fold higher, these data suggest that the ethyl ester is more effective in crossing the cell membrane since the relative potency as an anti-proliferative is approximately the same as the free acid.



Graph 7- Anti-proliferative assay of 4-methylthiobenzoylthioglycolic acid on DU 145 prostate cancer cells. The ethyl ester of this compound was also tested for comparison. Cells were grown to 50,000 cells per well and then treated or not treated with various concentrations of 4-methylthiobenzoyl thioglycolic acid or its ethyl ester. Growth was measured at 24, 48, 72, and 96 hours.

Anti-proliferation assay of S-(Phenylthioacetyl)thioglycolic acid

Graph 8 shows the results of the anti-proliferative assay with S-(phenylthioacetyl)thioglycolic acid. There is a significant inhibition of growth with this compound at concentrations 1.0 mM. Again, the concentrations exhibiting anti-proliferative activity preclude its use as an anti-proliferative in humans. In this experiment, a known growth inhibitor of DU 145 cells was tested as a



Graph 8- Anti-proliferative assay of S-(phenylthioacetyl)thioglycolic acid on DU 145 prostate cancer cells. 4-HPR was tested as a positive control. Cells were grown to 50,000 cells per well and then treated or not treated with various concentrations of S-(phenylthioacetyl)thioglycolic acid or 4-HPR. Growth was measured at 8, 24, 48, 72, and 96 hours.

positive control. 4-HPR completely inhibits cell growth in 48 hours at a concentration of 10 μ M, consistent with previously published results (Graph 8).

S-(4-Methylthiobenzoyl)thioglycolic acid and S-(phenylthioacetyl)thioglycolic acid were also tested since they showed the lowest inhibition constant against PAM. Since 4-HPR completely stopped the growth of the DU 145 cells and S-(4-methylthiobenzoyl) thioglycolic acid and S-(phenylthioacetyl)thioglycolic acid did not, it does not seem necessary to test the less potent inhibitors.

Conclusion

The anti-proliferative assays on S-(4-methylthiobenzoyl)thioglycolic acid and S-(phenylthioacetyl)thioglycolic acid did show a significant inhibition of growth, but only at high concentrations. The high concentration needed to effectively treat androgen-independent prostate cancer would require massive dosages if used to treat patients. Perhaps a compound with a lower inhibition constant would be more effective against the cells. These data suggest that a PAM inhibitor could be useful as an anti-proliferative drug, but compounds $> 10^3$ -fold more potent must be developed for anti-PAM drugs to even be considered for clinical use.

The kinetic constants are known for many substrates and inhibitors of PAM. Though none of the compounds bind tight enough to PAM to completely stop the growth of androgen-independent prostate cancer, they did show that they exhibit anti-proliferative activity. This shows that there is a potential that PAM inhibitors of considerably higher potency (lower K_i values) might have clinical relevance.

Since only the S-(thiolauroyl)thioglycolate bound at submicromolar concentrations, a new design should be developed. Instead of having substrate-like inhibitors, product-like or transition state analogs should be made. Preliminary data on some product-like inhibitors have showed potential in attaining this goal. More extensive kinetic studies on all of the inhibitors are required to fully understand the complexities of their interaction with PAM. Such data are necessary to completely exploit the specific interactions of this series of compounds with PAM to develop second-generation compounds that bind more tightly to PAM

More intensive molecular modeling of the inhibitors into the active site should be done. With the kinetic constants of these compounds and others previously done, a better database can be constructed for future compound development. The database will help predict which inhibitors will be most potent.

The next step in the anti-proliferative assays is to see if the compounds are actually inhibiting PAM. To do this, the amount of a particular amidated peptide hormone should be determined. If the compound is targeting PAM, there should be significantly less amount of the α -amidated hormone in the treated cancer cells compared to controls not exposed to the compound. The ethyl esters of current compounds need to be tested for esterase activity to see if they are getting cleaved within the cell. If they are not, then perhaps another functional group can be attached to the compounds to facilitate the crossing of the cell membrane. For example a benzyl ester might yield more promising results.

References

- Bell J; Ash D E; Snyder L M; Kulathila R; Blackburn N J; Merkler D J **Structural and functional investigations on the role of zinc in bifunctional rat peptidylglycine alpha-amidating enzyme.** *BIOCHEMISTRY* (1997), 36(51), 16239-46.
- Bertelsen A H; Beaudry G A; Galella E A; Jones B N; Ray M L; Mehta N M **Cloning and characterization of two alternatively spliced rat alpha-amidating enzyme cDNAs from rat medullary thyroid carcinoma.** *ARCHIVES OF BIOCHEMISTRY AND BIOPHYSICS* (1990), 279(1), 87-96.
- Bonkhoff H; Stein U; Remberger K **Androgen receptor status in endocrine-paracrine cell types of the normal, hyperplastic, and neoplastic human prostate.** *VIRCHOWS ARCHIV. A, PATHOLOGICAL ANATOMY AND HISTOPATHOLOGY* (1993), 423(4), 291-4.
- Bradbury A F; Finnie M D; Smyth D G **Mechanism of C-terminal amide formation by pituitary enzymes.** *NATURE* (1982), 298(5875), 686-8.
- Bundgaard H; Kahns A **Chemical stability and plasma-catalyzed dealkylation of peptidyl- α -hydroxyglycine derivatives – intermediates in peptide α -amidation.** *PEPTIDES* (1991), 12, 745-748.
- Eipper B A; Mains R E; Glembotski C C **Identification in pituitary tissue of a peptide alpha-amidation activity that acts on glycine-extended peptides and requires molecular oxygen, copper, and ascorbic acid.** *PROCEEDINGS OF THE NATIONAL ACADEMY OF SCIENCES OF THE UNITED STATES OF AMERICA* (1983), 80(16), 5144-8.
- Eipper B A; Mains R E **Recombinant DNA to study neuropeptide processing. General introduction.** *ANNUAL REVIEW OF PHYSIOLOGY* (1988), 50 305-7.
- Eipper B A; Stoffers D A; Mains R E **The biosynthesis of neuropeptides: peptide alpha-amidation.** *ANNUAL REVIEW OF NEUROSCIENCE* (1992), 15 57-85.
- Freeman J C; Villafranca J J; Merkler D J **Redox cycling of enzyme-bound copper during peptide amidation.** *JOURNAL OF THE AMERICAN CHEMICAL SOCIETY* (1993), 115(11), 4923-4.

- Jaron, S; Mains, R E; Eipper, B A; Blackburn, N J **The Catalytic Role of the Copper Ligand H172 of Peptidylglycine α -Hydroxylating Monooxygenase (PHM): A Spectroscopic Study of the H172A Mutant.** BIOCHEMISTRY (2002), 41(44), 13274-13282.
- Jones B N; Tamburini P P; Consalvo A P; Young S D; Lovato S J; Gilligan J P; Jeng A Y; Wennogle L P **A fluorometric assay for peptidyl alpha-amidation activity using high-performance liquid chromatography.** ANALYTICAL BIOCHEMISTRY (1988), 168(2), 272-9.
- Kyprianou N; English H F; Isaacs J T **Programmed cell death during regression of PC-82 human prostate cancer following androgen ablation.** CANCER RESEARCH (1990), 50(12), 3748-53.
- Landymore-Lim A E; Bradbury A F; Smyth D G **The amidating enzyme in pituitary will accept a peptide with C-terminal D-alanine as substrate.** BIOCHEMICAL AND BIOPHYSICAL RESEARCH COMMUNICATIONS (1983), 117(1), 289-93.
- Lee, H **Protein kinase C involvement in aloe-emodin- and emodin-induced apoptosis in lung carcinoma cell.** BRITISH JOURNAL OF PHARMACOLOGY (2001), 134(5), 1093-1103.
- Matthews D E; Piparo K E; Burkett V H; Pray C C **Animal Cell Technology: Products of Today, Prospects for Tomorrow** (Spier, R.E., Griffiths, J.B. and Bethold, W., Eds.) Butterworth-Heinemann Ltd., Oxford, U.K. (1994), 315-319.
- Merkler D J; Kulathila R; Tamburini P P; Young S D **Selective inactivation of the hydroxylase activity of bifunctional rat peptidylglycine alpha-amidating enzyme.** ARCHIVES OF BIOCHEMISTRY AND BIOPHYSICS (1992), 294(2), 594-602.
- Merkler, D J; **C-terminal amidated peptides: production by the in vitro enzymic amidation of glycine-extended peptides and the importance of the amide to bioactivity.** ENZYME AND MICROBIAL TECHNOLOGY (1994), 16(6), 450-6.
- Merkler D J; Kulathila R; Francisco W A; Ash D E; Bell J **The irreversible inactivation of two copper-dependent monooxygenases by sulfite: peptidylglycine α -amidating enzyme and dopamine β -monooxygenase.** FEBS LETTERS (1995), 366(2,3), 165-9.
- Merkler K A; Baumgart L E; DeBlassio J L; Glufke U; King L 3rd; Ritenour-Rodgers K; Vederas J C; Wilcox B J; Merkler D J **A pathway for the biosynthesis of fatty acid amides.** ADVANCES IN EXPERIMENTAL MEDICINE AND BIOLOGY (1999), 469 519-25.

Miller D A; Sayad K U; Kulathila R; Beaudry G A; Merkler D J; Bertelsen A H
Characterization of a bifunctional peptidylglycine alpha-amidating enzyme expressed in Chinese hamster ovary cells. ARCHIVES OF BIOCHEMISTRY AND BIOPHYSICS (1992), 298(2), 380-8.

Papsidero L D; Kuriyama M; Wang M C; Horoszewicz J; Leong S S; Valenzuela L; Murphy G P; Chu T M **Prostate antigen: a marker for human prostate epithelial cells.** JOURNAL OF THE NATIONAL CANCER INSTITUTE (1981), 66(1), 37-42.

Parker S L; Tong T; Bolden S; Wingo P A **Cancer statistics, 1996.** CA: A CANCER JOURNAL FOR CLINICIANS (1996), 46(1), 5-27.

Rocchi P; Boudouresque F; Zamora A J; Muracciole X; Lechevallier E; Martin P; Ouafik, L'Houcine. **Expression of adrenomedullin and peptide amidation activity in human prostate cancer and in human prostate cancer cell lines.** CANCER RESEARCH (2001), 61(3), 1196-1206.

Segel, I **Biochemical Calculations: How to Solve Mathematical Problems in General Biochemistry. 2nd Ed.** (1976), 448.

Southan C; Kruse L I **Sequence similarity between dopamine beta-hydroxylase and peptide alpha-amidating enzyme: evidence for a conserved catalytic domain.** FEBS LETTERS (1989), 255(1), 116-20.

Spector, T; Cleland, W W **Meanings of K_i for conventional and alternate-substrate inhibitors.** BIOCHEMICAL PHARMACOLOGY (1981), 30(1), 1-7.

Takahashi N; Ohba T; Togashi S; Fukui T. **Biological Activity of p-Methylaminophenol, an Essential Structural Component of N-(4-Hydroxyphenyl)retinamide, Fenretinide.** JOURNAL OF BIOCHEMISTRY (2002), 132(5), 767-74.

Tamburini P P; Young S D; Jones B N; Palmesino R A; Consalvo A P **Peptide substrate specificity of the alpha-amidating enzyme isolated from rat medullary thyroid CA-77 cells.** INTERNATIONAL JOURNAL OF PEPTIDE AND PROTEIN RESEARCH (1990), 35(2), 153-6.

Wilcox B J; Ritenour-Rodgers K J; Asser A S; Baumgart L E; Baumgart M A; Boger D L; DeBlassio J L; deLong M A; Glufke U; Henz M E; King L 3rd; Merkler K A; Patterson J E; Robleski J J; Vederas J C; Merkler D J **N-acylglycine amidation: implications for the biosynthesis of fatty acid primary amides.** BIOCHEMISTRY (1999), 38(11), 3235-45.